The contribution shift of ammonia-oxidizing archaea and bacteria to ammoxidation under Ag-NPs/SWCNTs/PS-NPs stressors in constructed wetlands

Yang, Xiangyu; Guo, Fucheng; Liu, Tao; He, Qiang; Vymazal, Jan; Chen, Yi

The contribution shift of ammonia-oxidizing archaea and bacteria to ammoxidation under Ag-NPs/SWCNTs/PS-NPs stressors in constructed wetlands

Xiangyu Yang [c,d], Fucheng Guo [a,b], Tao Liu [a,b], Qiang He [a,b], Jan Vymazal [e], Yi Chen [a,b,*]

[a] Key Laboratory of the Three Gorges Region's Eco-Environment, Ministry of Education, College of Environment and Ecology, Chongqing University, Campus B 83 Shabeijie, Shapingba, Chongqing 400044, China
[b] National Centre for International Research of Low-carbon and Green Buildings, Chongqing University, Chongqing 400044, China
[c] State Key Laboratory of Environmental Aquatic Chemistry, Research Center for Eco-Environmental Sciences, Chinese Academy of Sciences, Beijing 100085, China
[d] Department of Water Management, Sanitary Engineering, Faculty of Civil Engineering and Geosciences, Delft University of Technology, P.O. Box 5048, Delft 2600 GA, The Netherlands
[e] Department of Applied Ecology, Faculty of Environmental Sciences, Czech University of Life Sciences Prague, 16521 Prague 6, Czech Republic

ARTICLE INFO

ABSTRACT

Ammonia-oxidizing microorganisms (AOMs, archaea (AOA) and bacteria (AOB)) are primarily responsible for the ammoxidation in constructed wetlands (CWs). However, little is known about evaluating the response of AOA and AOB to engineered nanomaterials (ENMs) and quantifying the shift of their contribution to ammoxidation. Herein, we operated a series of CWs exposing to silver nanoparticles (Ag-NPs), single-walled carbon nanotubes (SWCNTs), and polystyrene nano-sized plastics (PS-NPs) with the wastewater-accumulating concentration of ENMs for 180 days. The results showed that the abundance of AOA *amo*A gene *in situ* was far lower than that of AOB, while the abundance ratio of AOA to AOB increased by 15 folds after 180-day experiment. Using DNA stable isotope probing (DNA-SIP) experiment, we found that the active AOB microbiota varied substantially but the AOA was more stable across different groups. Furthermore, the co-occurrence analysis proved that ENMs stress increased the negative coexistence pattern of AOA and AOB; predictive functional profiling showed that the ENMs enhanced the functional advantage of AOA by inhibiting AOB (mainly hydroxylamine oxidation process). Finally, the contribution of AOA increased under exposing to SWCNTs (18.35%), PS-NPs (24.92%), and Ag-NPs (32.14%) compared with control group (0.03%) for 180 days. Despite this, AOB was still the primary executant of ammoxidation in CWs. Overall, in our study, the differences in activities and contributions of AOMs were quantified in CWs, and a significantly negative coexistence relationship between AOA and AOB was revealed when exposed to emerging nanomaterials.

1. Introduction

In recent years, using engineered nanomaterials (ENMs, 1–100 nm in size) to solve environmental issues has become an inexorable trend [26]. For example, applications of ENMs in green chemistry, photocatalytic degradation of organic pollutants, remediation of polluted soils, water, or sediment, pollutant sensing, and detection, have been regularly reported. Additionally, the potential risks of ENMs have also been briefly discussed. Evaluating environmental concentration is a challenge for ENMs including metal, inorganic carbon, and plastics nanomaterials, which presently are estimated to occur in the environment and

wastewater at low (ng/L to mg/L) concentrations [15,18,19,25,31,38]. The ENMs are so stable that their degradation is not easily achievable, leading to many environmental toxicities.

Constructed wetlands (CWs) are an ecological water-treatment system and shore buffer zone that can effectively intercept 87%–98% of ENMs in wastewater [4,9,34]. However, with the accumulation of ENMs, the nitrogen-removing performance of CWs is gradually deteriorating, especially ammonia (NH_4^+-N) removal efficiency that has declined by approximately 50%–70% under more than a 60-day exposure [33,56,57]. NH_4^+-N heavy loading in CWs effluent can result in a series of environmental problems (e.g., eutrophication and ammonia

poisoning) [11,53]. Microbial nitrification is a mainstream dissimilatory pathway that oxidizes NH_4^+-N to hydroxylamine (NH_2OH) to nitrite (NO_2^--N) via ammonia-oxidizing microorganisms (AOMs, including archaea (AOA) and bacteria (AOB)) and finally to N_2 via denitrification [14,28]. However, when CWs are exposed to ENMs accumulation, who is the victim and what contributes to the shift in their ammonia-oxidation is still unclear.

Previous studies have reported that AOA had more contribution to ammonia-oxidizing process than AOB in natural wetlands [46]. On the one hand, AOA generally outnumbers AOB by approximately an order of magnitude [55,61]. On the other hand, the half-saturation constant of most of AOA for NH_4^+ (about 0.133 μM) was 2–4 orders of magnitude lower than other AOB strains [44], indicating AOA has a more intense affinity for NH_4^+-N and has competitive edges over AOB, particularly in infertile environments. However, unlike natural wetlands, in CWs, a high concentration of NH_4^+-N in influent creates an ideal condition for AOB growth. Furthermore, AOB had a much higher cell-specific ammonia-oxidizing activity and gene (i.e., *amo*ABC) abundance compared to AOA [6,17,51]; therefore, AOB was generally thought to be more a significant contributor than AOA in CWs. However, several groups of cell-specific activity data were used in research without rigorous consideration of the microbiota structure, which might cause unreliable results [55]. Some scientists have revealed the contribution differences of AOMs just using the inhibition experiments (e.g., acetylene, 1-octyne, sulfadiazine, dicyandiamide and antibiotics) [12,39,49]. In these experiments, AOA had a more ideal survival condition without the competition of AOB while it suffered a stronger inhibitory effect. Therefore, it could give a rough estimate of AOA and AOB activities but not accurately enough to clarify the difference in their activities and functions only using the inhibition experiment [54]. More progressive DNA-based stable isotope probe (DNA-SIP) technology has been utilized to explore active AOMs under exposing to ENMs. It is effective for differentiating the active AOMs while high-throughput sequencing results can obtain a clearer recognition of the community structures of active AOAs and AOBs [40,41]. The active cell-specific numbers and activities for AOMs can be reflected by effective gene abundance and microbiota structure, respectively. Based on this assumption, AOMs' ammonia-oxidizing capabilities can be comprehensively evaluated when exposing to the accumulation of the different ENMs in CWs.

In this study, we aimed to explore the contributions of AOA and AOB with and without exposure to different ENMs within CW systems. Three kinds of typical ENMs (silver nanoparticles (Ag-NPs), single-walled carbon nanotubes (SWCNTs) and polystyrene nanoplastics (PS-NPs)) were used to perform the disturbing experiments and for the first time answer i) how do AOA and AOB contribute to the ammoxidation in CWs, and how does the process change after exposure to ENMs? ii) what are the degrees of the effect of ENMs with different types of materials in regard to AOMs? and iii) how does the coexistence relationship of AOA and AOB change under the stress of ENMs? Answering these questions will provide important information needed to enhance the nitrogen removal in CWs and be of great significance to fully understand the effects of ENMs on natural nitrogen cycling.

2. Materials and methods

2.1. Preparation of engineered nanomaterials (ENMs)

Commercially produced polyvinylpyrrolidone (PVP)-coated silver nanoparticles (Ag-NPs) (purity: >99.99%), single-walled carbon nanotubes (SWCNTs) (purity: >95%), and polystyrene nanoplastics (PS-NPs) (5% w/v) were purchased from Sigma-Aldrich (St. Louis, MO, USA), XFNANO (Jiangsu, China), and Aladdin (Shanghai, China), respectively. During the experiments, each was diluted to 1 mg/L to create synthetic wastewater according to previous studies [47,56,60]. The ENMs within the synthetic wastewater was finely dispersed and homogeneous, and their morphologies were visualized using a transmission electron

microscope (TEM, JEM-1400, Tokyo, Japan) with diameters ranging from 50 to 80 nm (Fig. S1). The composition of synthetic wastewater was used to simulate the influents of WWTPs as described in the Supplementary Materials (Text S1). Briefly, it contained 200 mg/L of chemical oxygen demand (COD), 20 mg/L of NH_4^+-N, and 5 mg/L of total phosphorus (TP).

2.2. Experimental operation

Twelve subsurface-flow CW microcosms (4 sets × 3 replicates, with a length of 30 cm, a width of 30 cm, and a height of 50 cm) were constructed in a sequencing batch mode (hydraulic retention time = 5 days). All CW microcosms were filled with gravel (Φ: 8–10 mm, porosity: 0.4) and planted with cattail (*Typha latifolia*) [32]. The four systems containing non-ENMs-fed microcosms and three ENMs (Ag-NPs, SWCNTs, and PS-NPs) treated microcosms with environmental concentrations of 1 mg/L in wastewater were established in triplicate. The operation details are shown in the Supplementary Materials section (Text S2). The variations in the dissolved oxygen (DO) concentration as well as the pH of the synthetic wastewater in the CWs during one batch met the requirements needed for the experiment and are provided in Fig. S2. The experiment was performed for 180 days (36 batches). During the last batch all water samples were collected at different intervals from the pipe at a depth of 20 cm and were analyzed within 1 h after collection according to our standard methods [2]. Meanwhile, the assay of ammonia-oxidizing rates in all treatment groups were carried out by reducing NH_4^+-N to NO_2^--N and NO_3^-–N, and the detailed processes are with minor modifications according to Hurley et al. [22].

2.3. Ammonia-oxidizing microorganisms (AOMs) assay

2.3.1. ^{13}C-DNA stable isotope probing incubation

As shown in Fig. 1, after the 180-day exposure to ENMs, a total of 8 g of gravel was covered by a biofilm and sampled from three pre-set sampling columns from each CW microcosm (total of 9 samples for each CW microcosm, n = 9) in order to perform the DNA-SIP incubation. All samples were subjected to a pre-incubation to exhaust the residual substrates within the biofilm. Next, the wet gravel was transferred to a 100 ml conical flask to carry out DNA-SIP incubation using 50 ml of a synthetic solution according to the previous study [41]. The synthetic solution contained the same ENM concentration and was mixed with an equivalent amount of $NaH^{13}CO_3$ as the inorganic carbon source in all flasks. The details of synthetic solution composition and culture process are described in Supplementary Materials (Text S3). At the end of the incubation, the biofilm was stripped and frozen at −80 °C for the downstream analysis.

2.3.2. DNA extraction, isopycnic centrifugation and gradient fractionation

DNA from the biofilm samples was extracted using a Soil FastDNA SPIN Kit (MP Biomedicals, Solon, OH, USA) according to the manufacturer's protocol. The concentration and purity of the extracted DNA were detected using a Nanodrop lite UV spectrophotometer (Thermo Scientific, Waltham, MA) and stored at −80 °C. Equal masses of DNA from the duplicate ^{13}C-DNA experiments were combined to achieve a sufficient mass DNA (approximately 5 μg) for detecting and quantifiying the separated DNA. Next, the ^{13}C-labeling DNA solution was prepared and then subjected to centrifugation. The details of the centrifuged solutions composition and purification process are described within the Supplementary Materials (Text S3) according to Neufeld et al. [37]. Due to the poor concentration and quality of the obtained DNA (not shown in the data), the community structure and metabolic functions were analyzed based on the amplicon sequencing.

2.3.3. Quantitative PCR and high-throughput sequencing

After the 180-day experiment, quantitative PCR (qPCR) was performed using a MyiQ2 Real-Time PCR Detection System (Bio-Rad, USA)
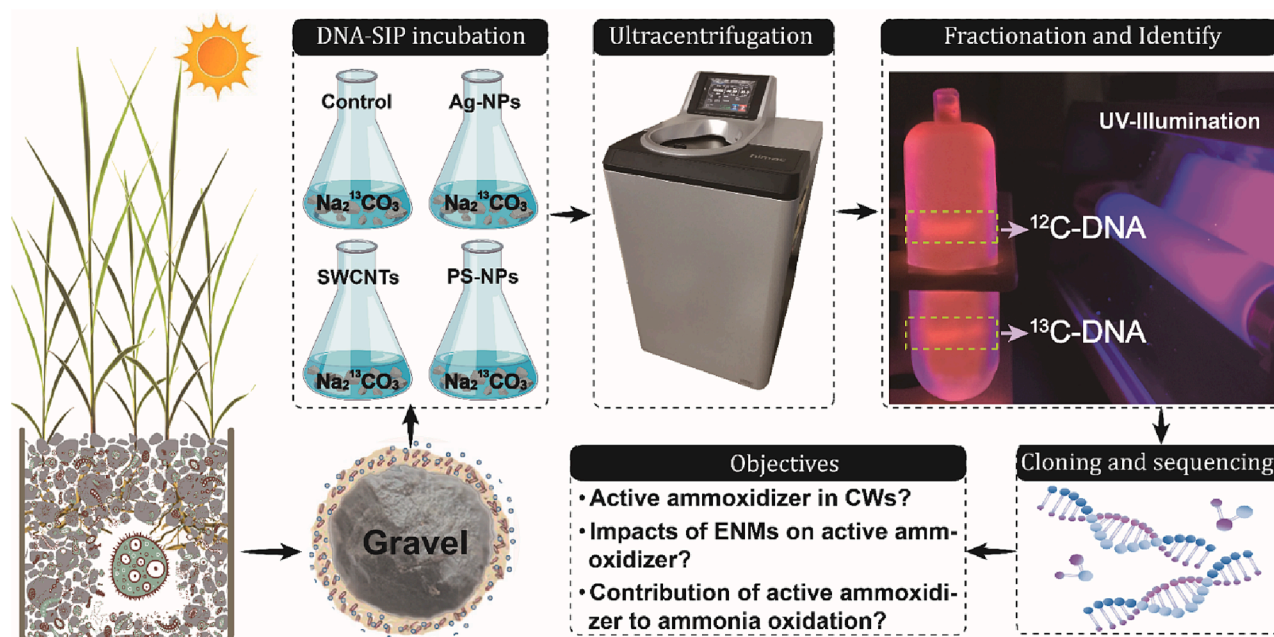
Fig. 1. The schematic diagram and objectives of experimental design concept of this study.

to quantify the abundance of AOA and AOB in the original biofilm. The ^{13}C-labeling DNA samples, the archaeal *amo*A gene (GenAOAF: 5′-ATAGAGCCTCAAGTAGGAAAGTTCTA-3′, the GenAOAR: 5′-CCAAGCGGCCATCCAGCTGTATGTCC-3′), the bacterial *amo*A gene (*amo*A-1F: 5′-GGGGTTTCTACTGGTGGT-3′, and the *amo*A-2R: 5′-CCCCTCKGSAAAGCCTTCTTC-3′ [K = G or T; S = G or C]) were targeted. The details are described in previous studies [36,43]. The composition of the reaction mixtures and the amplification details are described in the Supplementary Materials section (Text S4 and Table S1). The ^{13}C-labeling DNA was analyzed via the high-throughput sequence targeting V4-V5 regions of the archaeal/bacterial 16S rRNA gene using the primers 515F (5′-GTGYCAGCMGCCGCGGTAA-3′) and 926R (5′-CCGYCAATTYMTTTRAGTTT-3′), respectively. The raw data were removed barcodes and primer sequences and then imported into QIIME2 for the abundance table and taxonomy assignment [7]. Subsequently, the PCR amplification and the Illumina MiSeq sequencing were carried out by Majorbio (Shanghai, China).

2.4. Contribution shift of AOA and AOB

At the end of the 180-day experiment, the net ammoxidation efficiency was determined using the modified methods of Ouyang et al. [39]. Briefly, gravel samples (60 g) were collected according to the abovementioned method, and equally divided into three 100 ml serum bottles. These bottles were treated with: i) no amendment for control, ii) 6 μM aqueous concentration (Caq) of acetylene, and iii) 4 μM Caq of 1-Octyne. Acetylene treatment was set to block the ammonia-oxidizing and evaluate the acetylene-insensitive heterotrophic nitrification, and the 1-Octyne as the differential inhibitor acting on AOB was utilized to distinguish the contributions of AOA and AOB [39,50]. All serum bottles were incubated at 25 °C in the dark on a shaker at 100 rpm for 7.5 h. At the beginning and end of the incubation, active nitrogen (NH_4^+-N, NO_2^--N, and NO_3^--N) concentrations were measured. Finally, we utilized the results of the three treatment groups to determine the ammonia removal efficiency and the contribution ratio of AOA during the process of ammonia-oxidization using the following equations:

$$N_i = \frac{C_0 V_0 - C_i V_i}{C_0 V_0} \times 100\% \tag{1}$$

$$R_{AOA} = \frac{N_3}{N_1 - N_2} \times 100\% \tag{2}$$

where N_i is the ammonia removal efficiency of three treatment groups (i = 1, 2, and 3), C_0 and C_i are the initial and ending concentrations of the supernatant, V_0 and V_i are the initial and ending volume of the supernatant, and R_{AOA} is the contribution ratio of AOA to NH_4^+-N removal in biotic process.

2.5. Statistical analysis

The data assays were conducted in triplicate (n = 3), except for qPCR and high-throughput sequence (n = 9). The results are presented as the mean ± standard deviation. Analysis of variance (one-way ANOVA) was used to examine the significance of the results followed by the LSD post-hoc *t*-test, in which $P < 0.05$ is considered statistically significant (SPSS v.22.0, IBM). Co-occurrence network analysis and the phylogenetic investigation of communities via reconstruction of the unobserved states was conducted to analyse the coexistence patterns [Spearman's ρ > 0.8 (positive) or < -0.8 (negative) and $P < 0.01$] and the functional pathway profiles (PICRUSt2) of AOA and AOB based on the high-throughput sequence of the ^{13}C-labeling DNA samples. The details of script and database are described within our previous study [59], respectively.

3. Results

3.1. Ammonia-oxidizing performance of CWs

As shown in Fig. 2, the average removal efficiencies of NH_4^+-N in CWs were 55.4 % (Ag-NPs), 31.3 % (SWCNTs), 40.8 % (PS-NPs), and 36.2 % (control) after a 180-day accumulation (Fig. 2A). The majority of the NH_4^+-N was transformed into NO_2^--N or NO_3^--N, and the highest concentrations of the total NO_2^--N and NO_3^--N increased to 1.46 mg/L, 0.55 mg/L, 0.78 mg/L, and 0.80 mg/L for the control and ENMs treatments, respectively (Fig. 2B). The ammonia-removing efficiencies and the field of total NO_2^--N and NO_3^--N in all ENMs treatments were reflected in the TN removal. Those in the ENMs treatments were lower than those of the control group (Fig. 2C), which strongly indicated that the ammonia-oxidizing performances under ENM stress were lower than in control
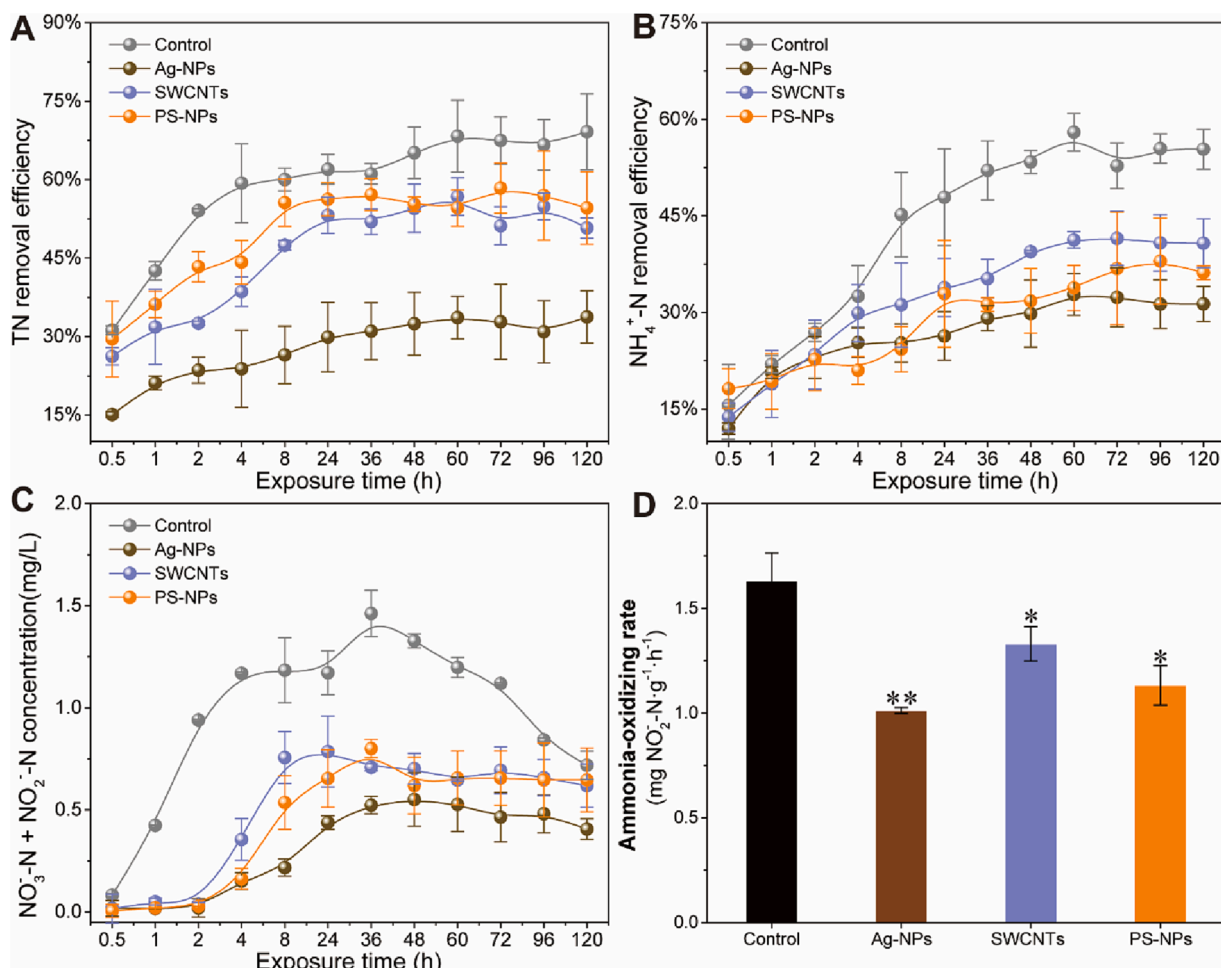
Fig. 2. Variations of removal efficiency of TN (A) and NH4 + -N (B) and the concentration changes of NO2--N + NO3--N production (C) and ammonia-oxidizing rate (D) in control and different ENMs treated CW microcosms during last batch of 180-day exposure. Asterisks (*) indicate the significant differences with control (n = 3, one-way ANOVA, *: $P < 0.05$, **: $0.01 < P < 0.01$, ***: $P < 0.01$).
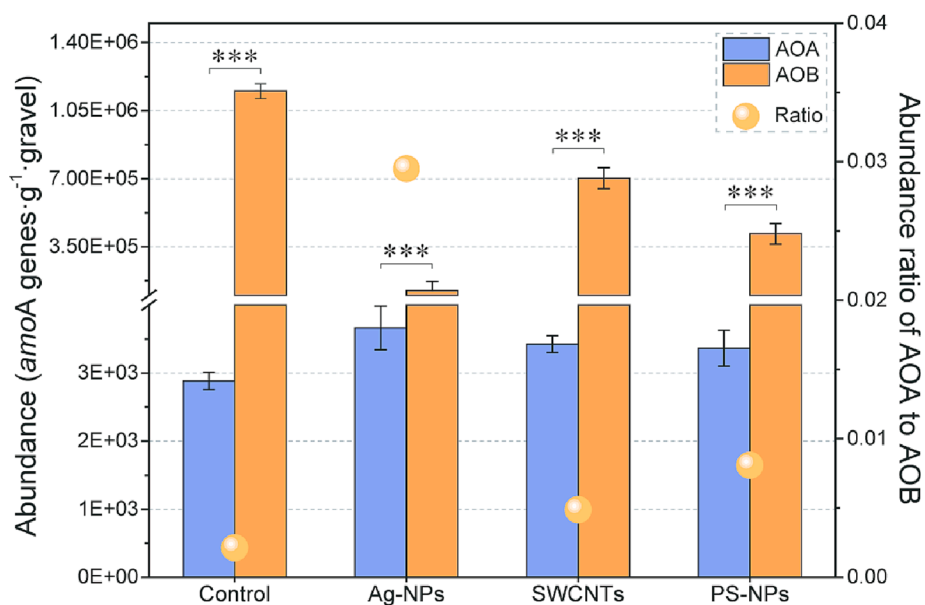
Fig. 3. Quantitative analyses of AOA and AOB abundance (column diagram) and the abundance ratio of AOA to AOB based on the qPCR of *amo*A gene *in situ* with different ENMs treatment in CWs. Asterisks (*) indicate the significant differences with control (n = 9, one-way ANOVA, $P < 0.01$).

group.

To further confirm the potential impacts of ENMs on microbial ammonia-oxidizing activity, a 7.5-h ammonia-oxidizing experiment was conducted after the 180-day feeding experiment. As shown in Fig. 2D, significant differences were observed between the control and the ENMs groups. The ammonia-oxidizing rates in the Ag-NPs, SWCNTs and PS-NPs treatment groups were 1.01, 1.33, and 1.13 mg·N·g^{-1}gravel·h^{-1}, and showed a decrease of 37.9%, 18.4%, and 30.6% compared to the control group (1.63 mg·N·g^{-1}gravel·h^{-1}) (Fig. 2D). The data demonstrated that the presence of the ENMs possessed significant negative impacts on the microbial ammonia-oxidizing process within the CWs, implying the strong sensitivity of AOMs to ENMs during a long-term accumulation.

3.2. In situ abundance of AOA and AOB in CWs

The abundance of AOA and AOB after the feeding experiment was determined by quantifiying the AOA and AOB *amo*A gene using qPCR. As shown in Fig. 3, compared to the control group, the copy numbers of the AOB *amo*A genes significantly decreased by 9.9-, 1.0-, and 2.2-fold in the Ag-NPs, SWCNTs and PS-NPs treatment groups, respectively. In contrast, the AOA *amo*A genes increased by 27.0 %, 18.8 %, and 16.7 % in the ENMs groups. The abundance ratio of AOA to AOB ranged from 0.002 to 0.029 in all groups. The lowest was seen in the control and the highest abundance ratio was in the Ag-NPs treatment group (Fig. 3). All data indicated that the AOB presented slight to no resistance no to the ENMs stress, while the AOA was not inhibited by ENMs accumulation in the CWs during long-term exposure. Although the abundance of AOB was much higher than that of the AOA, this did not illustrate which was active and contributed to ammoxidation.

3.3. DNA-SIP analysis of AOA and AOB

3.3.1. ENMs altered microbiota structure of AOA and AOB

In this study, DNA-SIP technology was used to determine who was primarily responsible for the ammoxidation between AOA and AOB as well as how much and what their contribution to ammoxidation was. After ultracentrifugation, the genes from the heavy fractions represented the active microbes, which might be responsible for ammoxidation [23,42]. Through the qPCR analysis, the ratios of the gene copy numbers of AOA *amo*A in ^{13}C-labeling DNA to AOB *amo*A were 0.0036 %–0.30 % in all treatments (Fig. S3). The ratio in the Ag-NPs treatment group was 83-fold higher than that in the control group. In the other treatment groups the ratios were also higher by 2.7- and 2.4-fold for the SWCNTs and the PS-NPs treatment groups compared to control, respectively (Fig. S3). Furthermore, the high-throughput sequencing of the ^{13}C-labeling DNA provided a clear understanding of the community structure of both the active AOAs and AOBs. For AOA, 11 species of AOA were detected and identified, and all of the species except *Nitrosopumilus_maritimus* showed higher community abundance in the ENMs treatment groups compared to the control group (Fig. 4A). Among them, *Nitrososphaera_gargensis*, *Nitrosopumilus_sp._NF5*, *Nitrososphaera_ever gladensis*, *Thaumarchaeota_archaeon_SCGC*, and *Thaumarchaeota_archaeon_MY3* showed the highest abundance under Ag-NPs exposure. Moreover, under SWCNTs stress, the *Nitrosoarchaeum_limnia* had the most apparent increase. The growth of *Nitrososphaera_viennensis* and *Nitrosopumilus* was more significant under PS-NP stress. In contrast, for the AOB species, the presence of ENMs significantly inhibited all 14 AOB community species. Moreover, the abundance of the AOB species decreased by 1.0%–93.4% (Fig. 4B). This data suggests that under ENMs stress the activity of AOB was more sensitive when compared to AOA.
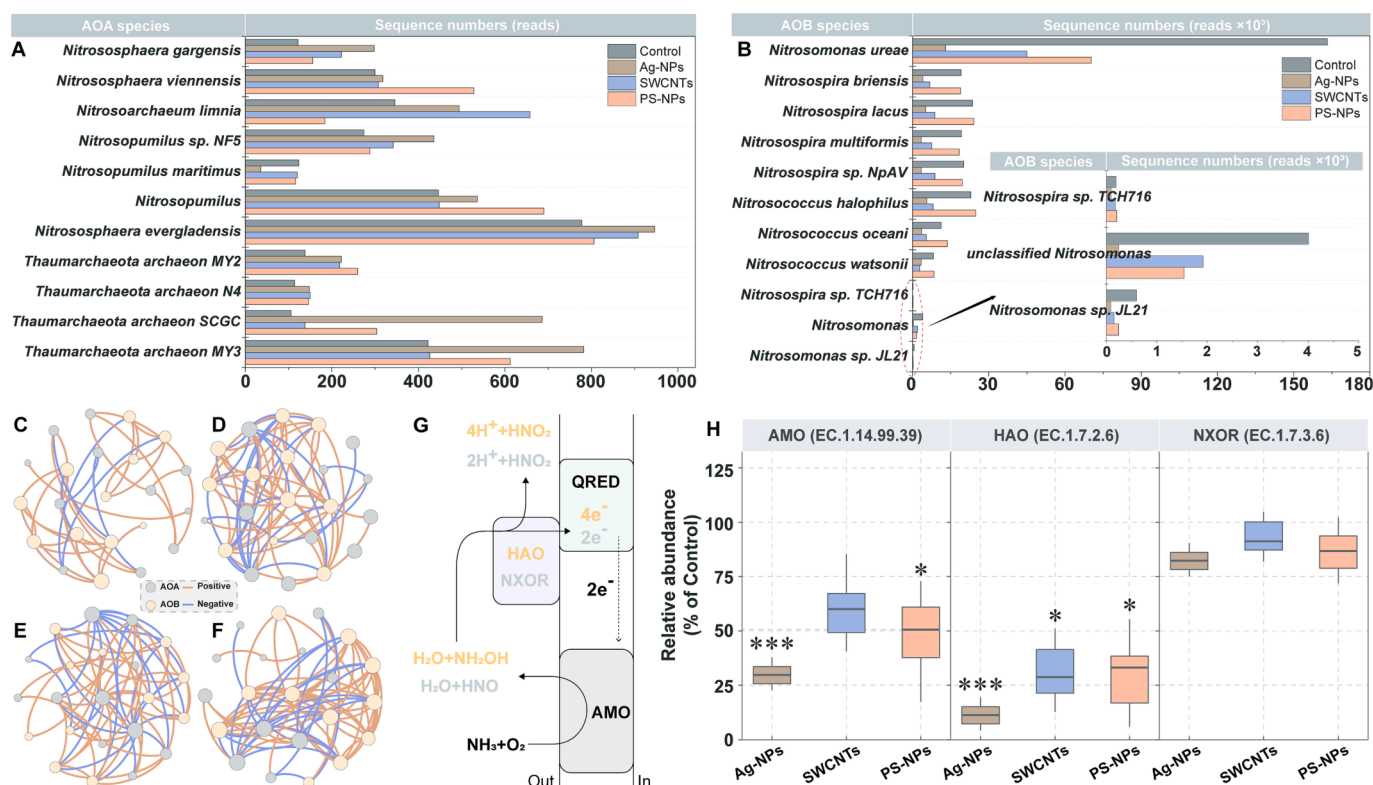
Fig. 4. Average sequence numbers of AOA (A) and AOB (B) at species level, co-occurrence networks (C: Control, D: Ag-NPs, E: SWCNTs, and F: PS-NPs), proposed AOA and AOB respiratory pathway (G), and functional predicted profiles (H) based on the high-throughput sequence of ^{13}C-labeling DNA samples. For each co-occurrence network, a connection between two nodes stands for a strong (ρ > 0.9) and significant (n = 9, P < 0.01) Spearman's rank correlation, and the size of each node is proportional relative weight (degree). For function predicted profiles, text indicates the described possible hydroxylamine (orange) and nitroxyl (gray) pathways, and asterisks (*) indicate the significant differences with control (n = 9, one-way ANOVA, ***: P < 0.01 and *: 0.05 < P < 0.01). (For interpretation of the references to colour in this figure legend, the reader is referred to the web version of this article.)

Compared to the abundance ratios of the AOA to AOB *in situ* biofilm samples (Fig. 3), the higher ratios of AOA to AOB were detected after the ^{13}C-labeling DNA-SIP incubation experiment, indicating that only one tenth of the AOBs were involved during the ammonia-oxidizing process while under ENM stress; therefore, the contribution of low abundance AOA might be underestimated.

3.3.2. ENMs reshaped the co-occurrence relationship of AOA and AOB

The overall non-random and ENMs-differentiated microbiota assembly patterns are demonstrated in the CW biofilm; thus, we further utilized the network model to uncover the underlying AMOs' co-occurrence patterns in all groups. Additionally, the three treatment groups, and their subnetworks contained 66 (Ag-NPs), 65 (SWCNTs), and 60 (PS-NPs) edges. All of edges in ENMs subnetworks were much higher than the subnetwork of the control group (28 edges) (Fig. 4C-4F). This pattern is consistent with the comparative profiles of the average degree as following: Control (1.68) < SWCNTs (2.89) < Ag-NPs (3.00) < PS-NPs (3.41) groups, reflecting that the ENMs affluxing into CWs promoted the frequency of AOMs' co-occurrence relationships. Furthermore, the co-occurrence patterns of all treatment groups were visually coloured according to AOMs of the network nodes (Fig. 4C-4F), facilitating the linking of associated AOMs' ecological niches to their taxonomic and functional profiles. Furthermore, compared with the control, various groups of positive and negative interactions among AOA or AOB thrived under various niches (as represented by the edge number) in different ENMs-treatment groups, indicating that niche differences between AOMs results from the ENMs stress influenced the community assembly and resulted in significant competition between AOA and AOB. Combined with the above results and based on the relative abundance and co-occurrence analysis of the ^{13}C-labeling DNA-SIP incubation, further consideration must be made regarding the actual contribution of AOA and AOB during the ammonia-oxidizing process when ENMs accumulation occurs in CWs.

3.3.3. ENMs selected for divergence in the functional profiles of AOA and AOB

The function potentials of ammoxidation of AOMs were predicted using PICRUSt2. In the ammonia metabolism pathway (Fig. 4G), the key genes (identified by EC number) coding key enzymes including ammonia monooxygenase (AMO, EC: 1.14.99.39), hydroxylamine oxidoreductase (HAO, EC: 1.7.2.6) for AOB [30], and nitroxyl oxidoreductase (NXOR, EC: 1.7.3.6) for AOA [52] were comparatively analyzed at the third-level of metabolic pathway in the KEGG dataset (Fig. 4H). The results showed that the three kinds of key enzymatic genes in all treatment groups decreased under ENMs stress over 180 days. Additionally, the AMO (EC: 1.14.99.39) enzymatic genes showed a significant decrease in Ag-NPs (31.3% of control, $P < 0.01$) and the PS-NPs (51.2% of control, $P < 0.05$) treatment groups (Fig. 4H). A significant decrease was observed in the HAO (EC:1.7.2.6) enzymatic genes, an AOB enzyme that decreased by 12.1% of control in the Ag-NPs group, 32.0% in the PS-NPs group, and 35.7% in the SWCNTs group, respectively. In contrast, NXOR, is a key AOA ammonia-oxidizing enzyme and had a slight decrease in all treatment groups. These results suggest that the accumulation of ENMs weakened the ammonia-oxidizing efficiency of CWs primarily through the inhibition of the AOB NH$_2$OH oxidizing process. Meanwhile no significant effect on the HNO oxidizing process of AOA was observed.

3.4. Contributions of AOA and AOB

After the 180-day experiment, the NH$_4^+$-N removal efficiency and contribution ratios of the active AOMs were determined through the inhibition experiment. As shown in Fig. 5, 34.5%–61.7% of NH$_4^+$-N removal was got by the biotic process (AOMs), with approximately 0.7%–1.6% being removed by the abiotic process (i.e., absorption or chemical process) in all treatment groups after 180-day experiment.

Furthermore, the contribution of active AOA to NH$_4^+$-N removal in biotic process increased by 18.35%–32.14%, and were 1108.3- (Ag-NPs), 632.8- (SWCNTs), and 859.3- (PS-NPs) fold higher than the control group (Fig. 5) using 1-Octyne inhibiting to AOB activity. These results suggested that under different ENMs exposure the more significant the decline of AOB activity was and the more remarkable the contribution ratio of active AOA was, which also implied that inhibiting AOB activity may provide better living conditions for AOA. Overall, the conclusions by the inhibition and DNA-SIP experiments co-reflected the differences in activities and contributions of AOA and AOB when exposed to emerging nanomaterials in CWs.

4. Discussion

Our research for the first time quantified the contribution of AOA and AOB in regard to the ammonia oxidizing process within ecological wastewater treatment systems. The results proved that the interference of ENMs reshaped the contribution structure by influencing the abundance of AOB and remodelling the coexistence relationship of AOA. These responses may also happen in other ecological medium when exposed to other biotoxic contaminants or under adverse conditions. However, in the complex water-purifying process it remains unclear whether ammoxidation is irrespectively or inconsiderably linked to AOA as implied by their exceptionally low abundance. Our research provides a detailed reference of this phenomenon.

The CW biofilm is cultured by means of feeding wastewater containing high level nutrients, where AOB generally outnumbers AOA [24]. Nevertheless, natural wetlands like the shore and marsh wetlands have much more AOA due to the poor nutrient concentrations [55]. In this study, the abundance of AOB far exceeded AOA in all CW microcosms during the 180-day experiment (Fig. 4A and 4B). In general, the ammonia-oxidizing process is completed by both AOA and AOB. In our study, the data showed that the microbial ammonia-oxidizing rate was significantly decreased under ENMs stress, resulting from the block of hydroxylamine oxidation process (Fig. 4H) and the decrease of the AOB abundance (Fig. 6A). Although the abundance of AOB decreased by 50% (in SWCNTs group) to 90% (in Ag-NPs group), the ammonia-removing efficiency only declined by an average 30% in ENMs treatment groups. We speculated that these results were due to (1) the surviving AOB has an excellent ammonia-oxidizing ability under exposing to ENMs [16]; (2) a colony of AOA has a huge potential to contribute to ammonia-oxidizing process [10].

To further confirm our hypotheses, the AOMs *amo*A genes were successfully labelled ^{13}C using a Na$_2^{13}$CO$_3$ incubation. During the DNA-SIP experiment and the high-throughput sequencing, we found that the ratio of active AOA and AOB in control group was different from all ENMs groups with AOB being the predominant AOM in all CWs. Similarly, Su et al. [48] also found that stimulating AOB activity can efficiently drive the ammonia-oxidizing rate in CWs. Furthermore, ENMs exposure significantly reduced AOB abundance, while a slight increase in AOA *amo*A genes was found. Why do AOA and AOB have different responses to long-term ENMs exposure in CWs? Generally, when AOB carries out the ammonia-oxidizing process, they first need to convert ammonium and O$_2$ into hydroxylamine, and then generate nitrite through the oxidation of hydroxylamine [32]. Half of the electrons obtained in this process are returned to ammonia-monooxygenase through cytochrome *c* (Cyto c) in order to complete the ammonium oxidation process [27]. The entire process is completed on the cell membrane, which is vulnerable to ENMs attack and destruction. In contrast, AOA lack the genes that encode Cyto c; thus, there is no transfer of electrons from the hydroxylamine oxidation process to the ammonia-oxidizing process in AOA [45]. Therefore, compared with AOB, AOA has a terser ammonia-oxidizing process and a shorter pathway, which might be the primary reason for the less (or no) impact on AOA exposing to ENMs accumulation. In addition, the results of the functional prediction based on 16S rRNA gene profiles confirmed that the genes coding to
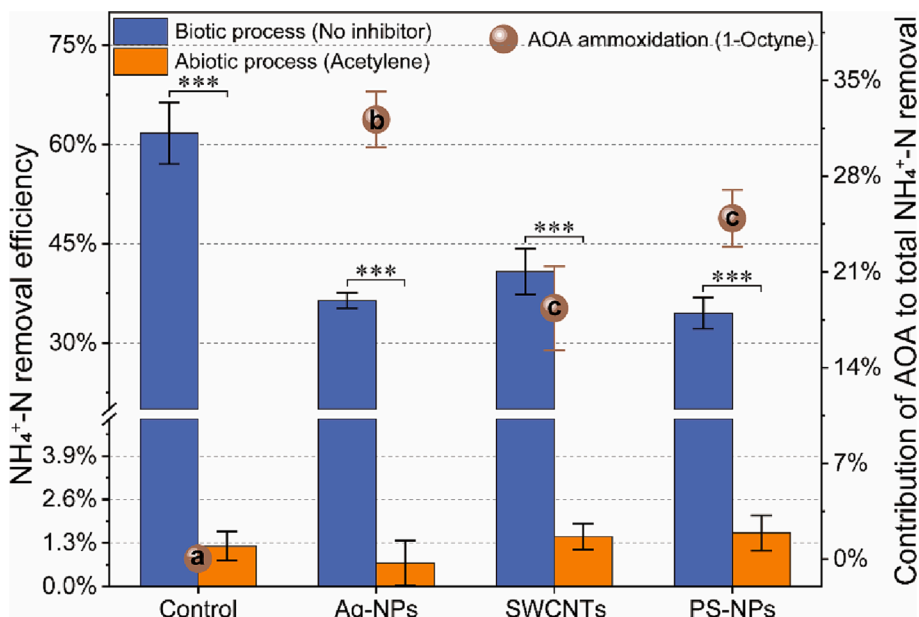
Fig. 5. The ammonia removal efficiencies under biotic and abiotic processes and the contribution of AOA to total ammoxidation after 180-day exposure to different ENMs. Asterisks (*) indicate the significant differences with control, and different letters (a, b, c) represent the significant differences at each treatment groups (n = 3, one-way ANOVA, $P < 0.05$).
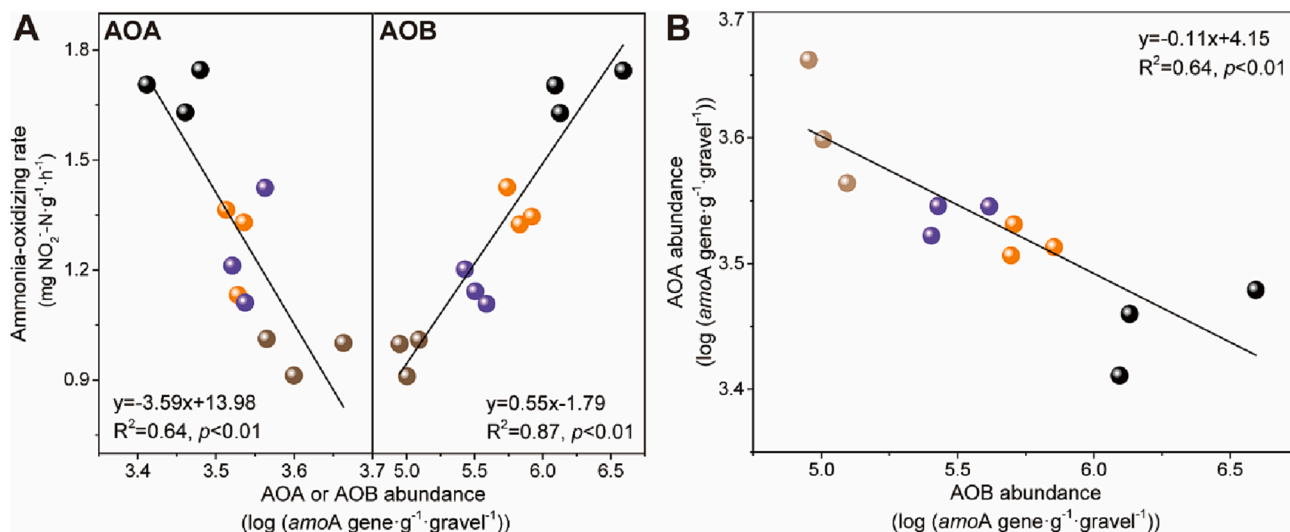

Fig. 6. Linear relationships between ammonia oxidation rate and AOMs abundance (A) and AOA abundance and AOB abundance (B) after ENMs feeding experiment. Different colors represent different treatment groups, black, pink, orange, and the brown are the control, SWCNTs, PS-NPs, and Ag-NPs treatment groups, respectively. (For interpretation of the references to colour in this figure legend, the reader is referred to the web version of this article.)

HAO in AOB was severely reduced, indicating that ENMs meddling ammoxidation is primarily due to the inhibition of the hydroxylamine oxidation pathway. The current analytical methods are still relatively difficult to confirm the differences in the ammonia metabolic, carbon fixing, and electron transferring processes in different AOMs; therefore, more studies on the binary culture system need to be performed to confirm the syntrophic or competitive mechanisms combined with advanced characterization and analysis methods (i.e., transcriptomics or proteomics) in the future.

It is known that archaea can often survive in extreme environments, unlike bacteria. For example, AOA can grow and successfully perform ammonia-oxidizing processes under a pH of <6.5, while AOB cannot accomplish this using its unique ammonia-oxidizing mechanism [1]; The growth temperature of AOA ranges from 0.2 °C to 97 °C, while AOB

belongs to mesothermal (10–25 °C) bacteria and their activity will be significantly inhibited or they will die when exposed to high temperatures [5,29]. In our study, the pH ranged from 7.4 to 7.8 (Fig. S2) and the temperature was approximately 25 °C in all the CWs during the 180-day experiment. Therefore, pH and temperature were not the reasons for the specific differences observed between the AOA and AOB. Oxygen is used as the substrate for the ammonia-oxidizing reaction. Due to the difference in oxygen affinity between AOA and AOB (AOA has better oxygen affinity) [62], the concentrations of the dissolved oxygen (DO) will affect the niche differentiation of AOA and AOB. Previous studies have found that the half satiation constant to the oxygen of AOA (0.3 nM – 10 µM) is far less than that of AOB (1.0 µM – 200 µM), thus AOA is more suitable for growth in a low oxygen environment [45]. In our study, the DO concentration of all wetland reactors greatly decreased from 7.5 mg/

L to 0.25 mg/L (7.8 μM) during the first 8 h in each batch (Fig. S2), which was more than the minimum half satiation constant of AOA and AOB. Therefore, DO was not the main factor that contributes to the low ammonia-oxidizing efficiency of AOMs.

As shown in Fig. 3, the more significantly the ENMs reduce the abundance of the AOBs, the higher the abundance ratio of AOA to AOB is. The questions are whether there is an antagonistic effect between AOB and AOB in wetland systems, whether the relative abundance of both AOMs remains balanced under this interaction, and whether this balanced coexistence is broken when adding ENMs needs to be answered. The answer to the first question has been confirmed by previous studies, which reported that bacteria can make enough space and food to survive by releasing bacteriocins that inhibit competitors in the environment [3,21,58]. In this study, we also found that AOA abundance was negatively correlated with the ammonia-oxidizing rate. The AOB abundance under exposure to ENMs (R = 0.64, $P < 0.01$) (Fig. 6), is consistent with the abovementioned conclusion. Meanwhile, the changes in co-occurrence patterns as well as the AOA to AOB ratio in different treatment groups further confirmed that the balanced coexistence of AOA and AOB was disturbed under ENMs stress within the CWs (Fig. 4C-F and S3), indicating that ammonia availability is not the only factor determining the abundance and distribution of AOA and AOB, ENMs stress can also change the ecological niches of AOMs. Furthermore, the ENMs could be as a selection pressure, which promoted an adaptive reconstruction of co-occurrence relationship between AOA and AOB. In the novel pattern, the more intensive co-occurrence pattern provided a more suitable and effective interaction relationships for metabolism, signal exchange and electronic transport among AOMs [59]. Overall, the gathering of ENMs in CWs possibly enhanced inter-specific interactions and created a novel niche for AOMs in CWs. As a result, the contribution of AOMs to ammoxidation was shifted while the coexistence was broken. Previous studies have also reported that AOA was the major contributor to the ammonia-oxidizing process in strongly acidic [63], high temperature (40 °C) [39], or no N-fertilizing [13] agricultural soils. Moreover, AOB dominated the ammonia-oxidizing process in cultivated agricultural soils and industrial wastewater treatment plants [41]. In our study, the contributions of AOA and AOB to ammoxidation in the CW system were first quantified by adding inhibitors. The data shows that AOA in all treatment groups were approximately 3000 cell·g^{-1}·gravel, accounting for only 0.5% (SWCNTs), 0.8% (NPs) and 3% (Ag-NPs) of all AOMs; however, their contribution to total ammonia-oxidation was as high as 18.4%–32.1%. These results shows that although the proportion of AOA was very low in all CW microcosms, their contribution to the ammonia-oxidizing process could not be ignored. Additionally, although the activity and abundance of AOB in the ENMs-treatment groups were significantly reduced, they were still the primary contributors of ammoxidation within the CW microcosms. Our results also indicated that when the CW systems suffered from the destruction of emerging contaminants, the degree of inhibition of the sensitive AOB might be underestimated because the recalcitrant AOA largely provided part of the ammonia-oxidizing efficiency. With respect to the metabolism process, the genome sequencing confirmed two Amt-type ammonium transporters, which could have unusually high affinity for ammonia [35]. The mechanistic information for the unprecedented capacity of ammonium acquisition and the metabolism pathway for its oxidation is still unknown. Hence, in order to further elucidate the interaction between AOA and AOB and the shift in the response mechanisms when exposed to external interventions, more studies of the binary culture system regarding the metabolism and electron transfer processes need to be performed to confirm the syntrophic or competitive mechanisms of AOA and AOB in the future. These findings extend the knowledge on the current understanding of the comprehensive partnerships of coordination among the AOM community in the ammonia-oxidizing process, which has broader implications in the fast selection and stabilization of AOMs in wastewater treatment, agricultural soil systems, as well as the general understanding of the ecology surrounding nitrogen cycling.

Considering that our study is based on the lab-scale wetlands, the operating parameters of each CW are unified with the sequencing batch model (5-day HRT) and the slightly fluctuating DO and pH (Fig. S2). Therefore, the influence of operating parameters on the performance of CWs and the activities of AOMs may be ignored in our experiment. In addition, the influent using synthetic wastewater tried to fully represent the real situation of the actual wastewater, there should be no specially selective effects on AOMs [20] in the control and treated CWs. Notably, in our DNA-SIP experiment, the ^{13}C-labeled inorganic carbon source (NaH^{13}CO$_3$) was used to label the genome of AOMs. Although there may be differences in the microbial assimilation of carbon source labelled/unlabelled the ^{13}C isotope [8], the effects resulting from those differences may be ignored in the long-term feeding process compared with the effects of ENMs [16]. Overall, in this study, the synthetic wastewater and molecular experiment have far less bias on the selectivity of AOMs than the responses of physiological activity brought by ENMs, and the experimental results and conclusions are reliable.

5. Conclusion

In this study, using the DNA stable isotope probing (DNA-SIP) experiment, the accumulation of ENMs for 180 days as a deterministic selection pressure was confirmed to drive the decrease in active AOB microbiota abundance and declined certain their ammonia-oxidizing processes (e.g., ammoxidation and hydroxylamine oxidoreduction) in CWs; In contrary, most of active AOA was increased in the microbiota abundance and functional gene (i.e., *amo*A). Based on the relative abundance and co-occurrence analysis, the results showed that the long-term accumulation of ENMs had an obvious effect on the AOMs niche in CWs, decreased the species segregation, and enhanced the co-occurrence relationship between AOA and AOB, as well as reshaped the actual contribution of AOA and AOB. In addition, in the inhibition experiment, we further proved that the contribution of active AOA to ammoxidation in biotic process increased when ENMs inhibiting to AOB activity [Ag-NPs (32.14%) > SWCNTs (18.35%) > PS-NPs (24.92%) > control group (0.03%)]. Although the possibility could not be ignored that the decline in nitrifying efficiency may put down to other abiotic mechanisms, the changes in microbiota structure, co-occurrence relationship and functional definitely underlie the overall obstructive impacts of ENMs on the ammoxidation process. Our findings of the ammonia-oxidizing performance and microbial mechanisms provides a novel insight into the ecotoxicological impacts of ENMs in CWs and how functional AOMs cope with the long-term environmental accumulation of ENMs.

Declaration of Competing Interest

The authors declare that they have no known competing financial interests or personal relationships that could have appeared to influence the work reported in this paper.

Data availability

Data will be made available on request.

Appendix A. Supplementary data

Supplementary data to this article can be found online at https://doi.

org/10.1016/j.cej.2023.142207.

References

[1] A. Aigle, C. Gubry-Rangin, C. Thion, K.Y. Estera-Molina, H. Richmond, J. Pett-Ridge, M.K. Firestone, G.W. Nicol, J.I. Prosser, Experimental testing of hypotheses for temperature- andpH-based niche specialization of ammonia oxidizing archaea and bacteria, Environ. Microbiol. 22 (9) (2020) 4032–4045.

[2] APHA, Standard methods for the examination of water and wastewater, 23rd ed., American Public Health Association, Washington, DC, 2017.

[3] N.S. Atanasova, M.K. Pietila, H.M. Oksanen, Diverse antimicrobial interactions of halophilic archaea and bacteria extend over geographical distances and cross the domain barrier, Microbiologyopen 2 (5) (2013) 811–825.

[4] H. Auvinen, V. Gagnon, D.P.L. Rousseau, G. Du Laing, Fate of metallic engineered nanomaterials in constructed wetlands: prospection and future research perspectives, Rev. Environ. Sci. Bio-Technol. 16 (2) (2017) 207–222.

[5] S. Barnard, M.W. Van Goethem, S.Z. de Scally, D.A. Cowan, P.J. van Rensburg, S. Claassens, T.P. Makhalanyane, Increased temperatures alter viable microbial biomass, ammonia oxidizing bacteria and extracellular enzymatic activities in Antarctic soils, FEMS Microbiol. Ecol. 96 (5) (2020).

[6] A.E. Bernhard, Z.C. Landry, A. Blevins, J.R. de la Torre, A.E. Giblin, D.A. Stahl, Abundance of ammonia-oxidizing archaea and bacteria along an estuarine salinity gradient in relation to potential nitrification rates, Appl. Environ. Microbiol. 76 (4) (2010) 1285–1289.

[7] E. Bolyen, J.R. Rideout, M.R. Dillon, N. Bokulich, C.C. Abnet, G.A. Al-Ghalith, H. Alexander, E.J. Alm, M. Arumugam, F. Asnicar, et al., Reproducible, interactive, scalable and extensible microbiome data science using QIIME 2, Nat. Biotechnol. 37 (8) (2019) 852–857.

[8] Brunner, B., Contreras, S., Lehmann, M.F., Matantseva, O., Rollog, M., Kalvelage, T., Klockgether, G., Lavik, G., Jetten, M.S.M., Kartal, B., et al., Nitrogen isotope effects induced by anammox bacteria. *Proc. Natl. Acad. Sci. U.S.A.*, **2013**, 110 (47), 18994–18999.

[9] M. Chen, D. Yang, F. Guo, R. Deng, W. Nie, L. Li, X. Yang, S. Liu, Y. Chen, Which sediment fraction mainly drives microplastics aging process: dissolved organic matter or colloids? J. Hazard. Mater. 443 (2023), 130310.

[10] X.-P. Chen, Y.-G. Zhu, Y. Xia, J.-P. Shen, J.-Z. He, Ammonia-oxidizing archaea: important players in paddy rhizosphere soil? Environ. Microbiol. 10 (8) (2008) 1978–1987.

[11] Y. Chen, Y. Wen, Q. Zhou, J. Vymazal, Effects of plant biomass on nitrogen transformation in subsurface-batch constructed wetlands: a stable isotope and mass balance assessment, Water Res. 63 (2014) 158–167.

[12] H.J. Di, K.C. Cameron, Inhibition of ammonium oxidation by a liquid formulation of 3,4-Dimethylpyrazole phosphate (DMPP) compared with a dicyandiamide (DCD) solution in six new Zealand grazed grassland soils, J. Soil. Sediment. 11 (6) (2011) 1032–1039.

[13] P. Duan, C. Fan, Q. Zhang, Z. Xiong, Overdose fertilization induced ammonia-oxidizing archaea producing nitrous oxide in intensive vegetable fields, Sci. Total Environ. 650 (2019) 1787–1794.

[14] P. Duan, Z. Wu, Q. Zhang, C. Fan, Z. Xiong, Thermodynamic responses of ammonia-oxidizing archaea and bacteria explain N2O production from greenhouse vegetable soils, Soil Biol. Biochem. 120 (2018) 37–47.

[15] M. Enfrin, J. Lee, Y. Gibert, F. Basheer, L. Kong, L.F. Dumee, Release of hazardous nanoplastic contaminants due to microplastics fragmentation under shear stress forces, J. Hazard. Mater. 384 (2020), 121393.

[16] J.-F. Gao, X.-Y. Fan, X. Luo, K.-L. Pan, Insight into the short-term effect of titanium dioxide nanoparticles on active ammonia oxidizing microorganisms in a full-scale wastewater treatment plant: a DNA-stable isotope probing study, RSC Adv. 6 (77) (2016) 73421–73431.

[17] J.-F. Gao, X.-Y. Fan, K.-L. Pan, H.-Y. Li, L.-X. Sun, Diversity, abundance and activity of ammonia-oxidizing microorganisms in fine particulate matter, Sci. Rep. (2016,) 6.

[18] F. Gottschalk, C. Lassen, J. Kjoelholt, F. Christensen, B. Nowack, Modeling flows and concentrations of nine engineered nanomaterials in the danish environment, Int. J. Environ. Res. Public Health 12 (5) (2015) 5581–5602.

[19] F. Gottschalk, T. Sun, B. Nowack, Environmental concentrations of engineered nanomaterials: review of modeling and analytical studies, Environ. Pollut. 181 (2013) 287–300.

[20] M. Harb, Y.H. Xiong, J. Guest, G. Amy, P.Y. Hong, Differences in microbial communities and performance between suspended and attached growth anaerobic membrane bioreactors treating synthetic municipal wastewater, Environ. Sci.-Water Res. Technol. 1 (6) (2015) 800–813.

[21] M.E. Hibbing, C. Fuqua, M.R. Parsek, S.B. Peterson, Bacterial competition: surviving and thriving in the microbial jungle, Nat. Rev. Microbiol. 8 (1) (2010) 15–25.

[22] S.J. Hurley, F.J. Elling, M. Koenneke, C. Buchwald, S.D. Wankel, A.E. Santoro, J. S. Lipp, K.-U. Hinrichs, A. Pearson, Influence of ammonia oxidation rate on thaumarchaeal lipid composition and the TEX86 temperature proxy, Proc. Natl. Acad. Sci. U.S.A. 113 (28) (2016) 7762–7767.

[23] Z. Jia, R. Conrad, Bacteria rather than Archaea dominate microbial ammonia oxidation in an agricultural soil, Environ. Microbiol. 11 (7) (2009) 1658–1671.

[24] Z. Jiang, S. Tang, Y. Liao, S. Li, S. Wang, X. Zhu, G. Ji, Effect of low temperature on contributions of ammonia oxidizing archaea and bacteria to nitrous oxide in constructed wetlands, Chemosphere 313 (2023).

[25] A.A. Keller, A. Lazareva, Predicted releases of engineered nanomaterials: from global to regional to local, Environ. Sci. Technol. Lett. 1 (1) (2014) 65–70.

[26] I. Khan, K. Saeed, I. Khan, Nanoparticles: properties, applications and toxicities, Arab. J. Chem. 12 (7) (2019) 908–931.

[27] M.M.M. Kuypers, H.K. Marchant, B. Kartal, The microbial nitrogen-cycling network, Nat. Rev. Microbiol. 16 (5) (2018) 263–276.

[28] Y.-P. Lin, A. Ansari, R.F. Wunderlich, H.-S. Lur, C. Thanh Ngoc-Dan, H. Mukhtar, Assessing the influence of environmental niche segregation in ammonia oxidizers on N2O fluxes from soil and sediments, Chemosphere (2022) 289.

[29] Z. Lin, W. Huang, J. Zhou, X. He, J. Wang, X. Wang, J. Zhou, The variation on nitrogen removal mechanisms and the succession of ammonia oxidizing archaea and ammonia oxidizing bacteria with temperature in biofilm reactors treating saline wastewater, Bioresour. Technol. 314 (2020).

[30] J.D. Lipscomb, A.B. Hooper, Resolution of multiple heme centers of hydroxylamine oxidoreductase from nitrosomonas.1. Electron-paramagnetic resonance spectroscopy, Biochemistry 21 (17) (1982) 3965–3972.

[31] H.H. Liu, Y. Cohen, Multimedia environmental distribution of engineered nanomaterials, Environ. Sci. Tech. 48 (6) (2014) 3281–3292.

[32] T. Liu, F. Guo, M. Chen, S. Zhao, X. Yang, Q. He, Silver nanoparticles disturb treatment performance in constructed wetlands: responses of biofilm and hydrophyte, J. Clean. Prod. 385 (2023).

[33] X. Liu, X. Yang, X. Hu, Q. He, J. Zhai, Y. Chen, Q. Xiong, J. Vymazal, Comprehensive metagenomic analysis reveals the effects of silver nanoparticles on nitrogen transformation in constructed wetlands, Chem. Eng. J. 358 (2019) 1552–1560.

[34] Y. Ma, J. Huang, T. Han, C. Yan, C. Cao, M. Cao, Comprehensive metagenomic and enzyme activity analysis reveals the negatively influential and potentially toxic mechanism of polystyrene nanoparticles on nitrogen transformation in constructed wetlands, Water Res. 117240 (2021).

[35] W. Martens-Habbena, P.M. Berube, H. Urakawa, J.R. de la Torre, D.A. Stahl, Ammonia oxidation kinetics determine niche separation of nitrifying Archaea and Bacteria, Nature 461 (7266) (2009) 976–U234.

[36] K.A. Meinhardt, A. Bertagnolli, M.W. Pannu, S.E. Strand, S.L. Brown, D.A. Stahl, Evaluation of revised polymerase chain reaction primers for more inclusive quantification of ammonia-oxidizing archaea and bacteria, Environ. Microbiol. Rep. 7 (2) (2015) 354–363.

[37] J.D. Neufeld, J. Vohra, M.G. Dumont, T. Lueders, M. Manefield, M.W. Friedrich, J. C. Murrell, DNA stable-isotope probing, Nat. Protoc. 2 (4) (2007) 860–866.

[38] B. Nowack, M. Baalousha, N. Bornhoeft, Q. Chaudhry, G. Cornelis, J. Cotterill, A. Gondikas, M. Hassellov, J. Lead, D.M. Mitrano, et al., Progress towards the validation of modeled environmental concentrations of engineered nanomaterials by analytical measurements, Environ. Sci.-Nano 2 (5) (2015) 421–428.

[39] Y. Ouyang, J.M. Norton, J.M. Stark, Ammonium availability and temperature control contributions of ammonia oxidizing bacteria and archaea to nitrification in an agricultural soil, Soil Biol. Biochem. 113 (2017) 161–172.

[40] K.-L. Pan, J.-F. Gao, X.-Y. Fan, D.-C. Li, H.-H. Dai, The more important role of archaea than bacteria in nitrification of wastewater treatment plants in cold season despite their numerical relationships, Water Res. 145 (2018) 552–561.

[41] K.-L. Pan, J.-F. Gao, H.-Y. Li, X.-Y. Fan, D.-C. Li, H. Jiang, Ammonia-oxidizing bacteria dominate ammonia oxidation in a full-scale wastewater treatment plant revealed by DNA-based stable isotope probing, Bioresour. Technol. 256 (2018) 152–159.

[42] J. Pratscher, M.G. Dumont, R. Conrad, Ammonia oxidation coupled to CO2 fixation by archaea and bacteria in an agricultural soil, Proc. Natl. Acad. Sci. U.S.A. 108 (10) (2011) 4170–4175.

[43] J.H. Rotthauwe, K.P. Witzel, W. Liesack, The ammonia monooxygenase structural gene amoA as a functional marker: Molecular fine-scale analysis of natural ammonia-oxidizing populations, Appl. Environ. Microbiol. 63 (12) (1997) 4704–4712.

[44] T. Sakami, Distribution of ammonia-oxidizing archaea and bacteria in the surface sediments of matsushima bay in relation to environmental variables, Microbes Environ. 27 (1) (2012) 61–66.

[45] C. Schleper, G.W. Nicol (2010) Advances in Microbial Physiology, Vol 57. Poole, R. K. (ed), pp. 1-41.

[46] A. Sims, J. Horton, S. Gajaraj, S. McIntosh, R.J. Miles, R. Mueller, R. Reed, Z. Hu, Temporal and spatial distributions of ammonia-oxidizing archaea and bacteria and their ratio as an indicator of oligotrophic conditions in natural wetlands, Water Res. 46 (13) (2012) 4121–4129.

[47] B. Steinhoff, J. Müller, D. Mozhayeva, B.T.F. Spelz, C. Engelhard, B. Butz, H. Schönherr, Investigation of the fate of silver and titanium dioxide nanoparticles in model wastewater effluents via selected area electron diffraction, Environ. Sci. Tech. 54 (14) (2020) 8681–8689.

[48] Y. Su, W.D. Wang, D. Wu, W. Huang, M.Z. Wang, G.B. Zhu, Stimulating ammonia oxidizing bacteria (AOB) activity drives the ammonium oxidation rate in a constructed wetland (CW), Sci. Total Environ. 624 (2018) 87–95.

[49] A.E. Taylor, K. Taylor, B. Tennigkeit, M. Palatinszky, M. Stieglmeier, D.D. Myrold, C. Schleper, M. Wagner, P.J. Bottomley, Inhibitory effects of C-2 to C-10 1-alkynes on ammonia oxidation in two nitrososphaera species, Appl. Environ. Microbiol. 81 (6) (2015) 1942–1948.

[50] A.E. Taylor, N. Vajrala, A.T. Giguere, A.I. Gitelman, D.J. Arp, D.D. Myrold, L. Sayavedra-Soto, P.J. Bottomley, Use of aliphatic n-alkynes to discriminate soil nitrification activities of ammonia-oxidizing thaumarchaea and bacteria, Appl. Environ. Microbiol. 79 (21) (2013) 6544–6551.

[51] M. Tourna, M. Stieglmeier, A. Spang, M. Koenneke, A. Schintlmeister, T. Urich, M. Engel, M. Schloter, M. Wagner, A. Richter, et al., Nitrososphaera viennensis, an ammonia oxidizing archaeon from soil, Proc. Natl. Acad. Sci. U.S.A. 108 (20) (2011) 8420–8425.

[52] C.B. Walker, J.R. de la Torre, M.G. Klotz, H. Urakawa, N. Pinel, D.J. Arp, C. Brochier-Armanet, P.S.G. Chain, P.P. Chan, A. Gollabgir, et al., Nitrosopumilus maritimus genome reveals unique mechanisms for nitrification and autotrophy in globally distributed marine crenarchaea, Proc. Natl. Acad. Sci. U.S.A. 107 (19) (2010) 8818–8823.

[53] K.S. Warren, S. Schenker, Liver disease and ammonia intoxication, *Gut* 4 (1963) 20–26.

[54] G. Wei, M. Li, W. Shi, R. Tian, C. Chang, Z. Wang, N. Wang, G. Zhao, Z. Gao, Similar drivers but different effects lead to distinct ecological patterns of soil bacterial and archaeal communities, Soil Biol. Biochem. 144 (2020).

[55] Y. Wei, Y. Lu, L. Xia, X. Yuan, G. Li, X. Li, L. Liu, W. Liu, P. Zhou, C.-Y. Wang, et al., Analysis of 2019 novel coronavirus infection and clinical characteristics of outpatients: An epidemiological study from a fever clinic in Wuhan, China, *J. Med. Virol.* 92 (11) (2020) 2758–2767.

[56] X. Yang, Q. He, F. Guo, X. Sun, J. Zhang, M. Chen, J. Vymazal, Y. Chen, Nanoplastics disturb nitrogen removal in constructed wetlands: responses of microbes and macrophytes, Environ. Sci. Tech. 54 (21) (2020) 14007–14016.

[57] X. Yang, Q. He, F. Guo, X. Sun, J. Zhang, Y. Chen, Impacts of carbon-based nanomaterials on nutrient removal in constructed wetlands: Microbial community structure, enzyme activities, and metabolism process, J. Hazard. Mater. 401 (2021), 123270.

[58] X. Yang, Q. He, T. Liu, F. Zheng, H. Mei, M. Chen, G. Liu, J. Vymazal, Y. Chen, Impact of microplastics on the treatment performance of constructed wetlands: Based on substrate characteristics and microbial activities, Water Res. 217 (2022).

[59] X. Yang, L. Zhang, Y. Chen, Q. He, T. Liu, G. Zhang, L. Yuan, H. Peng, H. Wang, F. Ju, Micro(nano)plastic size and concentration co-differentiate nitrogen transformation, microbiota dynamics, and assembly patterns in constructed wetlands, Water Res. 220 (2022).

[60] X.Y. Yang, Y. Chen, F.C. Guo, X.B. Liu, X.X. Su, Q. He, Metagenomic analysis of the biotoxicity of titanium dioxide nanoparticles to microbial nitrogen transformation in constructed wetlands, J. Hazard. Mater. 384 (2020).

[61] S. Yarwood, E. Brewer, R. Yarwood, K. Lajtha, D. Myrold, Soil microbe active community composition and capability of responding to litter addition after 12 years of no inputs, Appl. Environ. Microbiol. 79 (4) (2013) 1385–1392.

[62] Z. Yin, X. Bi, C. Xu, Ammonia-oxidizing archaea (AOA) play with ammonia-oxidizing bacteria (AOB) in nitrogen removal from wastewater, Archaea- Int. Microbiol. J. 2018 (2018).

[63] L.-M. Zhang, H.-W. Hu, J.-P. Shen, J.-Z. He, Ammonia-oxidizing archaea have more important role than ammonia-oxidizing bacteria in ammonia oxidation of strongly acidic soils, ISME J. 6 (5) (2012) 1032–1045.